5th International Conference on Biaxial/Multiaxial Fatigue and Fracture
Cracow'97, Poland

A. Varvani-Farahani* and T. H. Topper**

Biaxial Fatigue Crack Growth and Closure in SAE 1045 Steel

* Ph.D. student in Mechanical Engineering Department, University of Waterloo, Canada

** Professor of Civil Engineering Department, University of Waterloo, Canada

Keywords: Crack growth rate, strain intensity factor range, crack closure, fatigue life.

ABSTRACT- Crack growth and asperity induced closure mechanisms of biaxial fatigue cracks under constant amplitude loading and a load history having a periodic compressive overstrain were investigated. Biaxial fatigue tests were carried out using thin-walled SAE 1045 steel tubular specimens subjected to axial load and internal-external pressure.

Three biaxial principal strain ratios (axial strain/hoop strain) were used λ=-1 (pure shear loading), λ=-v (uniaxial loading), and λ=+1 (equibiaxial loading).

In the pure shear loading (λ=-1), surface cracks initially nucleated on slip bands at 45° to the axis of the specimen which coincides with the plane of maximum shear strain. Growth on the shear planes (microcracks) into the specimen occupied up to 90% of fatigue life during which time the surface length of the microcracks remained nearly constant. Failure then occurred by a rapid linking of microcracks at the end of a test.

In uniaxial loading (λ=-v), cracks initiated along the maximum shear plane at 45° to the surface of the specimen (Stage I growth) and failure then took place by Stage II growth perpendicular to the axis of the specimen.

In equibiaxial fatigue loading (λ=+1), cracks nucleated on the two maximum shear planes parallel and perpendicular to the specimen axis and propagated into the specimen on planes at 45° to the specimen surface.

Crack depth measurements were carried out using a Confocal Scanning Laser Microscope.

Crack opening stress measurements for biaxial fatigue cracks made using confocal scanning laser microscopy (CSLM) image processing of the crack profile, showed that the shear cracks and equibiaxial cracks were fully open at zero internal pressure for the in-phase periodic compressive overload histories. Therefore, there was no crack face interference and the strain intensity range was fully effective.

Introduction

Compared to the large volume of information on the growth of fatigue cracks under uniaxial loading conditions, experimental studies on fatigue crack propagation and closure in biaxial fatigue loading are comparatively rare in the literature. Some studies have been done on crack initiation and initial growth under biaxial fatigue loading, for instance, Parson and Pascoe [1] showed that crack initiation

and the direction of initial crack growth were dependent on the applied strain and biaxiality ratio. Brown and Miller [2] provided a comprehensive review of the literature on crack initiation and crack growth planes under biaxial loading. They considered nucleation and initial growth of fatigue cracks under torsion and biaxial tension and suggested the terms Case A and Case B cracks. In Case A (torsion) the initial crack growth was along the specimen surface however, in Case B (biaxial tension), cracks grew into the specimen. Socie [3] reviewed the cracking behaviour for different materials subjected to tension and torsion. He mapped them as different regions of A, B and C. For instance, in AISI 304 stainless steel, in torsional loading, region A behaviour was observed at short lives, in which failure occurred by a slow linking of initiated shear cracks. Region B was characterized by shear crack nucleation followed by crack growth on planes of maximum principal strain amplitude (Stage II planes). Region C was observed at the longest lives in torsion. Socie showed that under tensile loading, growth on the shear planes occurred by the propagation of a single crack rather than by a linking process (regions B and C).

However, there has been no quantitative study of the progress of a crack as it grows into the interior of the material.

This paper i) provides quantitative information concerning crack growth rates and shapes as a crack grows into the interior of the specimen under biaxial strain ratios (hoop strain/axial strain) of λ=-1, -v, and +1, ii) gives the effective (free closure) strain intensity factor range results, and iii) presents fatigue life under biaxiality ratios of λ=-1, -v, and +1 under constant amplitude loading and block loading histories containing periodic compressive overstrains.

Experimental procedure

Material and properties

The material examined in this investigation was SAE 1045 Steel in the form of as extruded 2.5 in diameter bar stock with the following chemical composition (Wt%): 0.46 C, 0.17 Si, 0.81 Mn, 0.027 P, 0.023 S, and the remainder Fe. This material is a medium carbon heat treatable steel which is widely used in the automotive industry. The microstructure of the SAE 1045 steel after final polishing showed pearlitic-ferritic features containing up to 30 μm long sulfide inclusions in the extrusion

direction. The modulus of elasticity is 206 GPa, the cyclic yield stress is 448 MPa. Uniaxial and biaxial fatigue specimen designs are given in Refs [4-5] respectively.

Short fatigue crack tests

Uniaxial loading

Uniaxial fatigue crack growth rate tests were performed in axial stress control on an MTS servo-hydraulic test machine with a load-cell capacity of 25000 Lb (111.20 KN). The crack growth tests under uniaxial constant amplitude loading (CAL) were performed with a stress amplitude of 138 MPa (R=-1). Periodic compressive overload crack growth tests were performed with compressive overloads of -300 MPa, -360 MPa, and -430 MPa followed by number of small cycles of n=50, 200, 500, and 1000 [4].

Fatigue life tests were performed under strain control for both uniaxial constant amplitude loading and load histories containing periodic overloads. The number of small cycles per block was adjusted to keep the overload damage at about 20% of the total damage. Figs.1a -1b illustrate the load history of uniaxial (CAL) and block loading history containing periodic compressive overloads (PCO) tests.

Biaxial (shear) loading

A series of thin-walled tubular specimens were cyclically loaded in the axial direction in the load frame while pressure was alternately applied to the inside and outside of the specimen during each cycle. The biaxial fatigue machine is described in Ref. [5].

Constant amplitude biaxial fatigue tests and tests with load histories containing periodic compressive overstrains (PCO) were performed in strain control at a frequency of 0.5 Hz, and zero mean strain (R=-1). The axial strain (ε_a) and transverse (hoop) strain (ε_h) were controlled to provide a 180° out-of-phase biaxial strain ratio of λ=-1. Figs.1c-1d present the load histories used for biaxial fatigue tests under constant amplitude loading and the histories having blocks of a periodic compressive overload followed by n small cycles. The number of small cycles per block was adjusted to keep the overload damage at about 20% of the total damage.

Shear crack length was measured using an optical microscope at the same intervals as depth measurements were performed using a confocal scanning laser microscope (CSLM).

Equibiaxial fatigue loading

Equibiaxial fatigue tests were performed under strain control for both constant amplitude loading and tests with load histories containing periodic overstrains. The axial strain and hoop strain were controlled to provide an in-phase biaxial strain ratio of λ=+1.

Figs 1c-1f illustrate the load histories of equibiaxial fatigue tests under constant amplitude loading and the histories having blocks of a periodic compressive overload followed by n small cycles.

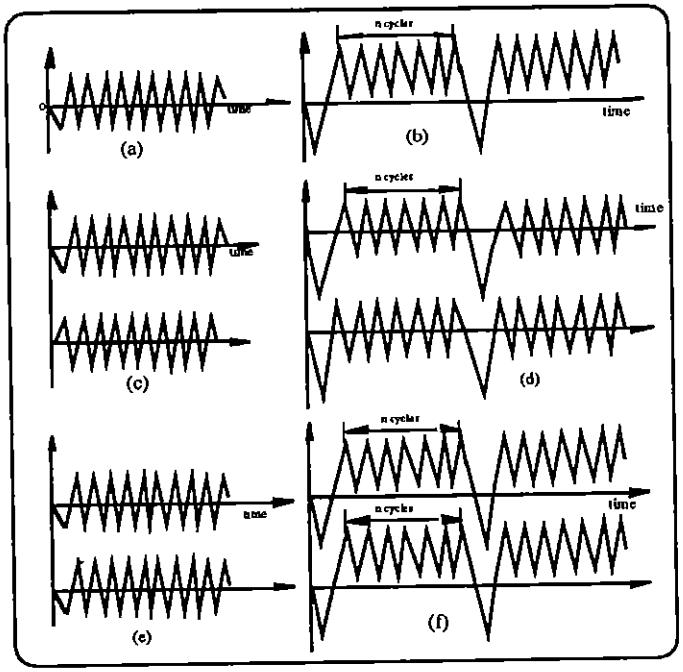

Fig.1 Fatigue test block histories under constant amplitude and load histories containing periodic compressive overstrains, a and b) uniaxial loading, c and d) shear loading, and e and f) equibiaxial loading.

Biaxial crack opening stress measurements

Fatigued tubular specimens were pressurized internally using a hydraulic device in the confocal scanning laser microscope. Hoop and axial stresses due to a progressive increase in the static internal pressure opened the crack along the maximum shear plane and three dimensional images of the crack

were acquired using a confocal scanning laser microscope (CSLM). The CSLM apparatus and measurements were described in detail in previous studies [6-7].

Results and discussion

Crack initiation and growth

Uniaxial fatigue loading (λ=–v)

Under a uniaxial loading condition, cracks first initiated and grew into the specimen on the maximum shear plane at 45° to the specimen surface (Stage I growth). After growing through one or two grains in Stage I, the crack plane rotated to become normal to the axis of loading (Stage II growth).
Fig 2 illustrates the plane and direction of initial growth of a crack under uniaxial loading.

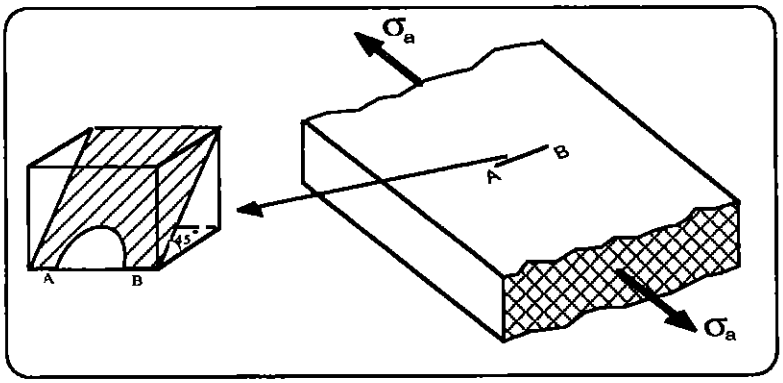

Fig.2 Plane of crack initiation and initial growth under uniaxial loading (λ=–v).

Biaxial shear cracks (λ=-1)

In 180° out-of-phase biaxial loading (λ=-1) tests on tubular specimens, shear cracks initially nucleated on an active slip band system which coincided with the maximum shear planes at ±45 degrees to the axial direction of the specimen. Microcracks (shear planes) propagated into the surface of the specimen while their length remained unchanged.

Fig 3 shows the plane of maximum shear strain and the direction of initial growth of shear cracks. The shear strain (γ) is equal to the difference of axial and hoop strains (ε_a-ε_h).

Microcracks of 3 μm initiated along the plane of maximum cyclic shear strain at fractions of specimen fatigue life (N/N_f) of 0.05, 0.11, 0.095, and 0.09 at shear strain amplitudes of 0.3%, 0.4%, 0.6%, and 1.0%, respectively.

The propagation of microcracks which initiated along slip bands (on the maximum shear plane) can be characterized as R-system crack behavior using the terminology introduced first by Marco and Starkey [8]. In this system, cracks start at many points on a specimen and progress toward the interior of the material (depth direction).

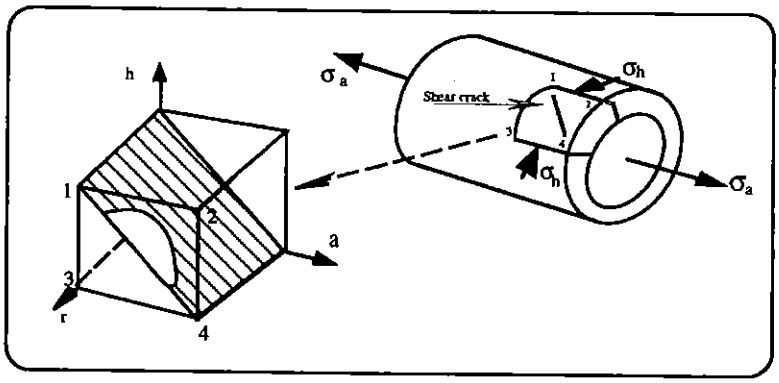

Fig.3 Plane of crack initiation and initial growth under shear fatigue loading (λ=−1).

The number of microcracks increased as cycling progressed. Once a crack initiated, its surface length did not increase much until the specimen reached about 90% of its fatigue life. However cracks grew into the specimen as the number of cycles increased. For the first 90% of the fatigue life, the microcracks grew along the maximum shear plane in the depth direction while the surface crack length remained nearly unchanged. These microcracks were uniformly distributed on the surface of specimen. At 60%-70% of the fatigue life, linking up of a few microcracks was observed (Fig. 4a). At 90%-95% of the fatigue life a progressive growth of microcracks by a linking up on shear planes was observed (Fig. 4b). Failure occurred shortly thereafter by a rapid linking up of microcracks (Fig. 4c).

At higher shear strain amplitudes, microcracks appeared to be more open and more distinct than at lower strain amplitudes.

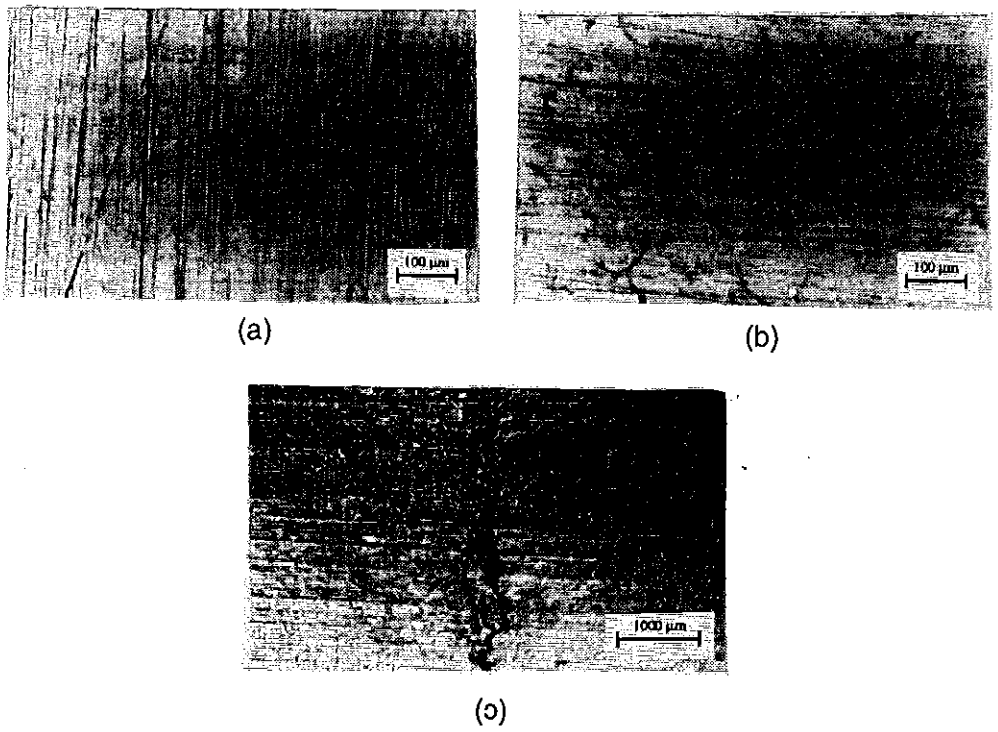

Fig. 4 Crack growth under shear loading a) linking up of a few shear microcracks at 60-70% of the fatigue life, b) linking up of many shear microcracks at 90-95% of the fatigue life, and c) failure after a rapid linking of shear microcracks.

Equibiaxial fatigue cracks (λ=+1)

In equibiaxial (in-phase biaxial) fatigue tests on tubular specimens, cracks initiated and grew along the specimen surface on the two maximum shear planes parallel and vertical to the specimen axis and propagated into the specimen on planes at 45° to the specimen axis. Fig.5 shows the plane of crack initiation and initial growth of an equibiaxial fatigue crack (λ=+1).

Equibiaxial cracks initiated on the planes of maximum shear strain at fractions of specimen fatigue life (N/N_f) of 0.074, 0.088, 0.086, 0.083, and 0.085 at biaxial strain amplitudes of 0.10%, 0.135%, 0.15%, 0.22% and 0.30% respectively.

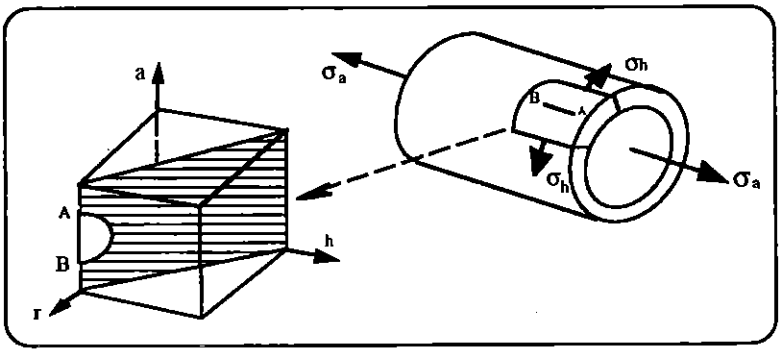

Fig.5 Plane of crack initiation and initial growth under equibiaxial loading (λ=+1).

Vertical equibiaxial cracks initiated at several points on the tubular specimen and propagated along and into the specimen. In most of tests, failure defined by oil leaking through the specimen thickness occurred when the crack length exceeded of 2 mm. Fig.6 shows photos of initial growth and failure of equibiaxial fatigue cracks.

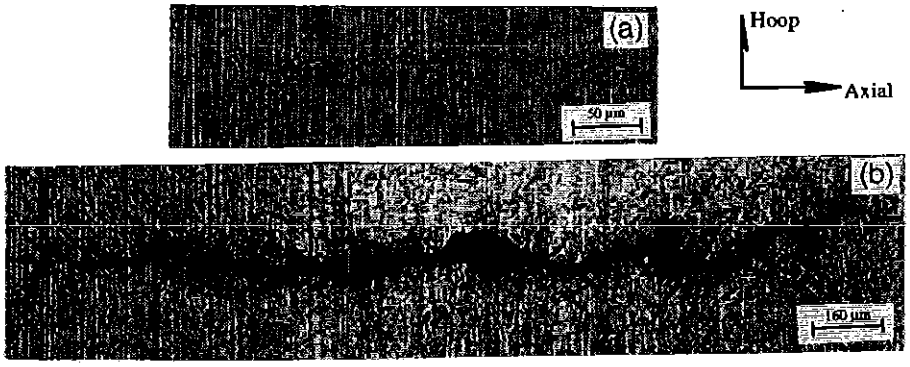

Fig.6 Micrographs of a) initial growth and b) failure under equibiaxial fatigue loading.

Biaxial crack growth mechanism

Biaxial shear cracks (λ=-1)

After, a crack initiated it became more distinct as the number of cycles increased but, there was no significant increase in the surface crack length. The crack depth along the initiation plane measured from a defined initiation depth of 3 μm on the slip plane (which coincided with the maximum shear plane) increased.

The propagation of microcracks along the plane of crack initiation occupied 90-95% of the fatigue life. This portion of life was followed by a rapid linking of microcracks leading to failure. Figure 7 shows crack depth versus cycles data for constant amplitude tests of the tubular 1045 steel specimen under shear loading from initiation to failure. The solid part of the curves corresponds to crack growth on the plane of maximum shear strain and the dashed part of the curves corresponds to the period of rapid linking up of microcracks (shear planes) at the end of a test.

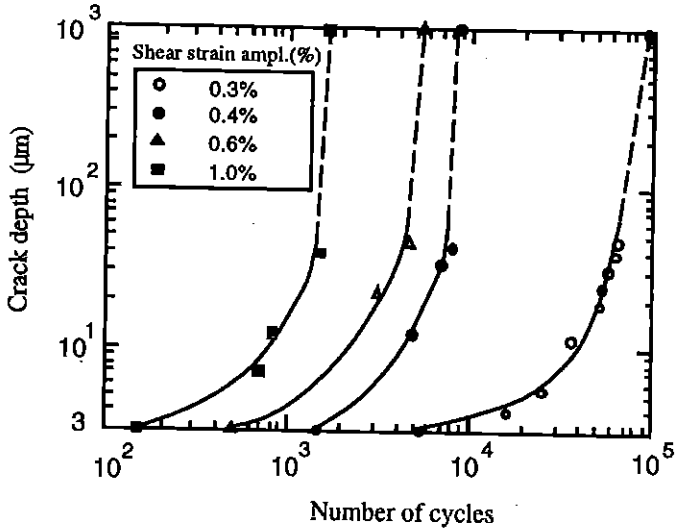

Fig.7 Crack growth results along the crack plane as the number of cycles changes.

Equibiaxial fatigue cracks (λ=+1)

The growth mechanism of cracks created under in-phase biaxial fatigue loading (λ=+1) is different from that for 180° out-of-phase biaxial fatigue loading (λ=-1). In equibiaxial fatigue loading, once a crack initiated (3 μm in depth), its surface length and depth increased as the number of cycles increased. Failure occurred when the surface crack length exceeded of 2 mm. Fig.8 presents the crack depth measurement results on the plane of maximum shear strain as the number of cycles increase. These results show that as the magnitude of the strain amplitude increases, cracks grow faster into the specimen surface.

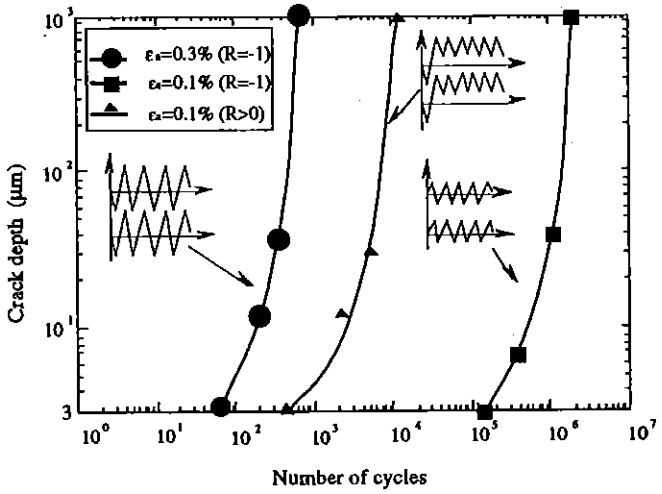

Fig.8 Crack growth results from initiation to failure under equibiaxial CAL and PCO fatigue loading.

The variation of aspect ratio (a/c) with crack depth in both λ=-1 and λ=+1 are given in Fig.9.

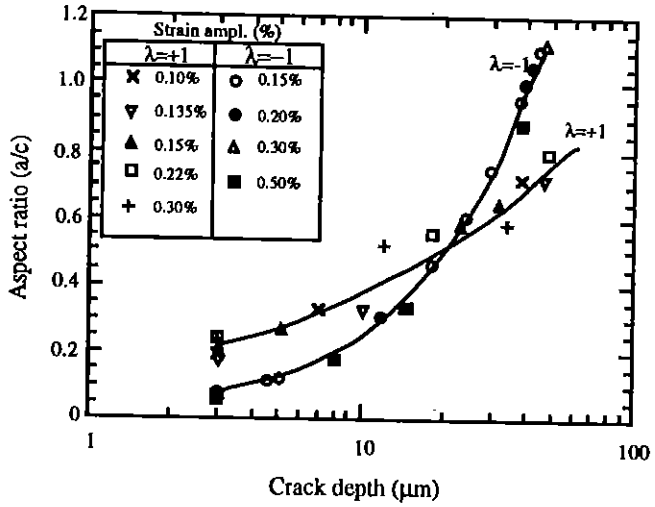

Fig.9 Crack aspect ratio versus the crack depth for both λ=-1 and λ=+1.

In biaxial shear loading, the initiation, initial growth and coalescence of cracks on planes of maximum shear strain occupied up to 90% of the fatigue life and then failure occurred by a rapid linking of shear planes (see Fig.10a). However, in equibiaxial fatigue loading, once a crack initiated, it grew on the length and depth directions until failure took place (see Fig.10b).

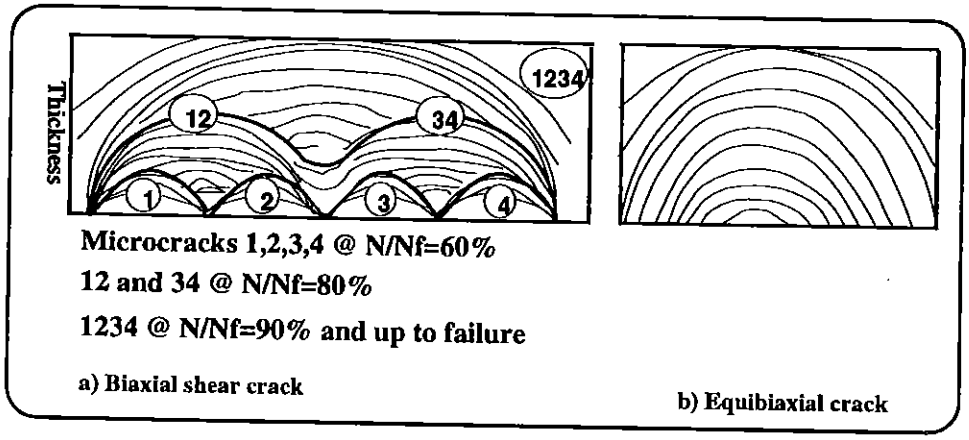

Fig.10 Schematic presentation of biaxial fatigue crack growth mechanism a) biaxial shear cracks, and b) equibiaxial fatigue crack.

The growth of uniaxial and biaxial fatigue cracks under constant amplitude loading and load histories containing compressive overloads

Irwin [9] derived K-factor for an embedded elliptical crack under uniform tension based on the stress field around an ellipsoidal cavity proposed by Green and Sneddon [10]:

$$K = \frac{\sigma\sqrt{\pi a}}{\Phi}\Psi \tag{1}$$

where Φ is the elliptic integral:

$$\Phi = \int_0^{\pi/2}\left[1-\left(1-\left(\frac{a}{c}\right)^2\right)\mathrm{Sin}^2\varphi\right]^{1/2} d\varphi \tag{2}$$

where φ is the angle in the parametric equation of an ellipse, parameter Ψ is a function of aspect ratio (a/c) and angle φ and expressed as:

$$\Psi = \left(\mathrm{Sin}^2\varphi + \left(\frac{a}{c}\right)^2 \mathrm{Cos}^2\varphi\right)^{1/4} \tag{3}$$

Kassir and Sih [11] solved K-factor for a flat elliptical crack subjected to a shear loading:

$$K_{Shear} = \frac{\tau\sqrt{\pi a}}{B\,\Psi}(1-\nu)\left(1-\left(\frac{a}{c}\right)^2\right)\mathrm{Sin}\,\varphi \tag{4}$$

where the parameter B is a function of aspect ratio and Poisson's ratio and is expressed as:

$$B = \left[\left(1-\left(\frac{a}{c}\right)^2\right)-\nu\right]\Phi + \nu\left(\frac{a}{c}\right)^2 L \tag{5}$$

where L for shear loading is :

$$L = \int_0^{\pi/2}\left[1-\left(1-\left(\frac{a}{c}\right)^2\right)\mathrm{Sin}^2\varphi\right]^{-1/2} d\varphi \tag{6}$$

Geometry factors F_G for cracks under uniaxial and equibiaxial loading and geometry factor $F_{G(II)}$ for a crack under shear loading were obtained respectively from eqn(1) and eqn (4) as:

$$F_G = \frac{\Psi}{\Phi} \tag{7-a}$$

$$F_{G(II)} = \frac{(1-\nu)}{B\,\Psi}\left(1-\left(\frac{a}{c}\right)^2\right)\mathrm{Sin}\,\varphi \qquad (7\text{-b})$$

Socie et al [13] used the same analysis for strain intensity factor range of small cracks under tension, torsion and mixed mode loading conditions.

Strain intensity factor range values were calculated for short fatigue cracks under uniaxial and equibiaxial fatigue loading using eqn (8a).

$$\Delta K = F\,Q\,\Delta\epsilon\;E\sqrt{\pi a} \qquad (8\text{-a})$$

where, ΔK is the strain intensity factor range, Q is the surface strain concentration factor [12], $\Delta\epsilon$ is the strain range (R=-1), E is the elastic modulus, and a is the crack depth.

Similarly, the strain intensity factor range was calculated for a semi-elliptical surface crack under biaxial (shear) using eqn (8b):

$$\Delta K_{II} = F_{II}\,Q\,\Delta\gamma\;G\sqrt{\pi a} \qquad (8\text{-b})$$

where $\Delta\gamma$ is the shear strain range (R=-1), G is the shear modulus, and a is the crack depth on the plane of maximum shear strain. The strain concentration factor Q is a function of crack size and grain diameter D which is given by eqn (9)[12].

$$Q = 1 + 5.3\exp\left(-\alpha\frac{a}{D}\right) \qquad (9)$$

Where α is a factor that represents the ease of cross-slip in the material.

Correction factors F and F_{II} (in eqn (8)) are expressed by:

$$F = F_G\,F_S \qquad (10\text{-a})$$

$$F_{II} = F_{G(II)}\,F_S \qquad (10\text{-b})$$

Subscripts G and S in eqns (10 a-b) correspond to geometry and surface corrections and F_S=1.12 was used as surface crack correction.

The crack growth rate for the small cycles in the uniaxial and biaxial overload test histories, was obtained by subtracting the crack growth due to the compressive overstrain cycle from the growth per block due to the periodic compressive overloads followed by n small cycles and dividing by the number of small cycles per block.

$$\left(\frac{da}{dN}\right)_{Small} = \frac{n+1\left(\frac{da}{dN}\right)_{Total} - \left(\frac{da}{dN}\right)_{Overloads}}{n} \qquad (11)$$

For uniaxial loading crack growth tests, it was shown [4] that a periodic compressive overload of -430 MPa (near the yield stress) increases the crack growth rate dramatically. It was also shown that the application of a compressive overload above -430 MPa did not result in an additional increase in crack growth rate. Similarly, Kemper et al [14] and Tack and Beevers [15] reported a saturation in crack growth rate when the magnitude of compressive overload increases beyond of a certain level.

In this study, saturation in the crack growth rate due to a periodic compressive overload of -430 MPa corresponds to fully open crack and a fully effective strain intensity crack growth rate.

The crack growth rate of small cycles calculated using eqn (11) is plotted in Fig.11 against strain intensity factor ranges calculated using eqn (8).

Fig. 11 presents an effective strain intensity factor range (ΔK_{eff})-$(da/dN)_{small}$ curve obtained from a uniaxial load history having periodic compressive overloads of near yield point magnitude.

The value of the uniaxial effective strain intensity factor range at the threshold was found to be 2.50 MPa$\sqrt{m}$.

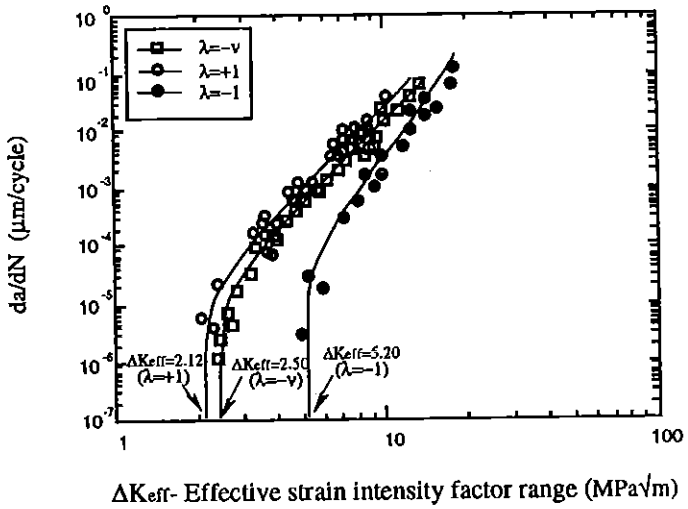

Fig. 11 Effective strain intensity factor range versus crack growth rates for uniaxial and in-phase biaxial PCO fatigue tests of λ=+1 and λ=−1 ratios.

Crack opening stress measurements for biaxial fatigue cracks made using confocal scanning laser microscopy (CSLM) image processing of the crack profile, showed that the shear cracks and equibiaxial cracks were fully open at zero internal pressure for the in-phase periodic compressive overload histories. Therefore, there was no crack face interference and the strain intensity range was fully effective. The crack growth rate for small cycles was calculated using eqn (11) and plotted in Fig.11 versus the strain intensity factor range calculated from eqns (8a-8b). Fig. 11 also presents fully effective ΔK-da/dN curves for shear and equibiaxial fatigue cracks under load histories containing in-phase periodic overstrains of near yield point magnitude.

The effective value of strain intensity factor (near the threshold) for biaxial (shear) fatigue loading (λ=-1) and equibiaxial fatigue loading (λ=+1) were found to be 5.20 and 2.12 MPa$\sqrt{m}$ respectively.

Fatigue life

Fatigue life-strain amplitude data plotted in Fig.12a show that the fatigue strength is reduced by a factor that ranged from 1.24 at short lives to 3.37 at long lives when periodic compressive overloads of near yield point magnitude are applied in uniaxial tests. The corresponding reductions in the biaxial (shear) fatigue strength vary from 1.40 to 1.70 (Fig 12b).

Equibiaxial fatigue strength was reduced by a factor that ranged from 1.65 at short lives to 2.5 at long lives when periodic compressive overstrains of near yield point magnitude are applied (Fig.12c)

The uniaxial strain-life data are compared with biaxial life-strain data for SAE1045 steel. To this end, the strain-life curves are compared on the base of octahedral shear strain, defined as:

$$\frac{\gamma_{oct}}{2} = \frac{1}{2}\left[(\varepsilon_1 - \varepsilon_2)^2 + (\varepsilon_2 - \varepsilon_3)^2 + (\varepsilon_3 - \varepsilon_1)^2\right]^{1/2} \qquad (12)$$

where ε_1, ε_2, and ε_3 are the principal amplitude strains.

Fig. 12d presents the number of cycles to failure versus the octahedral shear strain amplitude for the uniaxial and biaxial constant amplitude loading. Fig.12d shows that the octahedral shear strain approach gives a reasonable correlation between the uniaxial and in-phase (λ =+1) and 180° out-of-phase (λ =-1) biaxial fatigue life data.

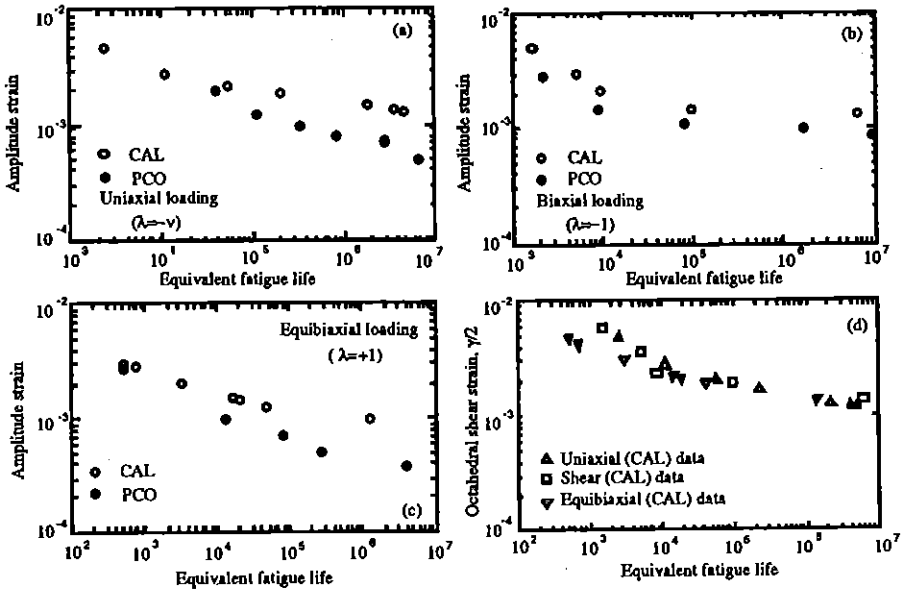

Fig.12 Fatigue life data under uniaxial and biaxial fatigue loading.

Conclusions

1. In uniaxial fatigue loading (λ=-v), cracks initiated along the maximum shear plane at 45° to the surface of the specimen (Stage I growth) and failure then took place by Stage II growth perpendicular to the axis of the specimen. In biaxial shear loading (λ=-1), the initiation , initial growth and coalescence of planes of maximum shear strain occupied up to 90% of the fatigue life and then failure occurred by a rapid linking of shear planes. However, in equibiaxial fatigue loading (λ=+1), once a crack initiated, it grew on the length and depth direction until failure took place.

2. Crack depth growth results obtained using confocal scanning laser microscopy revealed that as the biaxial strain amplitude increased the crack growth rate on the shear planes increased and an

application of a periodic compressive overstrain of -0.3% led to an acceleration of crack initiation, crack growth rate and failure.

3. The application of the in-phase periodic compressive overstrain opened the crack completely through its mouth and depth and therefore there was no crack face interference and the strain intensity range was fully effective. The threshold strain intensity factor range for biaxial shear loading and equibiaxial loading were found to be 5.2 and 2.12 MPa$\sqrt{m}$ respectively.

4. There was a reduction in fatigue strength which varied from about 1.24 in short lives to about 3.37 in long lives (10^7 cycles) when the periodic compressive overload of the magnitude of yield stress was applied. This reduction for biaxial (shear) fatigue strength varied from 1.40 to 1.70 and for equibiaxial fatigue strength ranged from 1.65-2.50 for the same equivalent number of cycles.

References

[1] Parson, M.W. and Pascoe, K. J. (1976), Observation of surface deformation, crack initiation and crack growth in low-cycle fatigue under biaxial stress, Mater. Sci, Engng, vol.22, pp.31-50

[2] Brown, M. W. and Miller, K. J., (1973), A theory for fatigue failure under multiaxial stress strain conditions, Proceedings, Institute of Mechanical Engineers, vol.187, pp.745-755

[3] Socie, D. (1993) in 'Advances in Multiaxial Fatigue', ASTM STP 1191, McDowell, D. L. and Ellis, R. (Eds), American Society for Testing and Materials, Philadelphia, 7-36

[4] Varvani-Farahani, A. and Topper, T. H. (1996), in 'Proceedings of the sixth international fatigue congress (Fatigue 96)'., Lutjering, G. and Nowack, H. (Eds), vol.1, pp.295-300, Berlin, Germany

[5] A Varvani-Farahani and T. H. Topper (1997) "Crack Growth Measurements of Shear Cracks Under Constant Amplitude and Biaxial Loading and Periodic Compressive Overstraining in 1045 Steel", Submitted to the International Journal of Fatigue.

[6] A Varvani-Farahani, T. H. Topper, and A. Plumtree (1996), " Confocal Scanning Laser Microscopy Measurements of the Growth and Morphology of Microstructurally Short Fatigue Cracks in Al 2024-T351 Alloy", Fatigue and Fracture of Engineering Materials and Structures. Vol. 19, pp.1153-1159

[7] A Varvani-Farahani and T. H. Topper (1997) "Short Fatigue Crack Characterization and Detection Using Confocal Scanning Laser Microscopy (CSLM)", Accepted for publication in ASTM STP 1318.

[8] Marco, S. M. and Starkey, W. L. (1954), Transaction of ASME, vol. 76, pp.627-632

[9] Irwin, G. R. (1962), Crack extension force for a part-through crack in a plate, Journal of Applied Mechanics, Transaction of ASME , vol. 29, pp.651-654

[10] Green, A. E. and Sneddon, I. N. (1950), The stress distribution in the neighborhood of a flat elliptical crack in an elastic solid, Proc. Cambridge Phil. Soc., vol.46, pp.159-164

[11] Kassir, M. K. and Sih, G. C. (1966), Three-dimensional stress distribution around an elliptical crack under arbitrary loadings, Journal of Applied Mechanics, Transaction of ASME , vol. 33, pp.601-611

[12] Abdel-Raouf, H., Topper, T. H., and Plumtree, A. (1992), International Journal of Fatigue, vol. 14, pp. 57-62
[13] Socie, D. F., Hua, C. T., and Worthem, D. W. (1987), Mixed mode small crack growth, Fatigue Fract. Engng Mater. Struct., vol.10, pp.1-16
[14] Kemper, H., B. Weiss, and R. Stickler (1989), An alternative presentation of the effect of the stress ratio on the fatigue threshold. Engineering Fracture Mechanics, vol.32, pp.591-600
[15] Tack, A. J. and C. J. Beevers (1990), The influence of compressive loading on fatigue crack propagation in three aerospace bearing Steels. In Proc. 4th Int. Conf. on Fracture and Fatigue Thresholds, (H. Kitagawa and T. Tanaka, eds), Vol.II, pp.1179-84 , MCEP Ltd, Honolulu.

Acknowledgment-The first author wishes to thank the Ministry of Culture and Higher Education of Iran for a scholarship.